

Polynomial Description of the Topological Invariant in Inhomogeneous Superconducting Wires

Marcos Pérez^{1,*} and Gerardo Martínez^{1,2}

¹*Instituto de Física, UFRGS, 91501-970 Porto Alegre-RS, Brazil*

²*Instituto de Física Teórica UAM/CSIC, Madrid, Spain*

(Dated: December 14, 2024)

We present universal features of topological superconducting wires. Periodic site modulations are used to study the effect of distributed potentials. An integer polynomial description is achieved by splitting the topological invariant in two parts, dependent/independent of the chemical potential. For the homogeneous case, an elliptical region is found where the topological invariant oscillates. The zeros of these oscillations occur at points where the fermion parity switches for finite wires. Enhancement of these oscillations with the inhomogeneity leads to new non-topological phases.

PACS numbers: 71.10.Pm, 03.65.Vf

Introduction.— Topological phases arising in superconducting materials have become a major research topic in condensed matter physics in the recent years [1–3]. Indeed, the search for Majorana zero modes have already begun [4]. The potential applications of these quantum phases are sustained by their robustness against a weak disorder, suggesting thus its realization in fault tolerant quantum computing [5, 6]. In this work, we deal with this scenario by implementing some spatial modulations that could mimic disorder effects in such topological phases.

A paradigmatic model in this context is the Kitaev chain [7], a lattice version of a spinless p -wave superconducting wire, whose topological phase has a bulk gap protected by time-reversal and particle-hole symmetries. This model has been broadly studied, including spatial modulations [8–15], and its basic properties are well known. Moreover, further complex cases with symmetry breaking interactions, like spin-orbit or quartic fermionic terms, have been proposed to discuss more recent experiments [16–18]. Yet, the key ingredients of the Kitaev free model enable us to deal with universal aspects of the topology with or without interactions, since all strongly interacting topological phases can be represented by non-interacting systems [19–21].

In order to approach the above picture with aspects of disorder, we study analytical properties of the topological invariant after the inclusion of inhomogeneities. In this Letter, we build up a description of the topology with integer polynomials that emerges as a consequence of periodic spatial modulations. Such iconic result reproduces analytically most effects of the inhomogeneities for this kind of models and may become an important starting point to study disorder in these systems.

There are some previous works that study the case of modulated chemical potentials [8–14], using a transfer matrix approach and, as far as we know, one work deals with a modulated hopping [15], using the enlarged unit cell explored here. They found, exploiting among other tools a scaled chemical potential [9, 10], that the shape of spatial distributions modify the original topological

phase diagram of the Kitaev model. Here, we are able to describe the origin of those changes by introducing a topological invariant which is characterized by an oscillatory polynomial delimited by two values. The behavior of the oscillatory part and its delimiting complements fairly describe the changes induced on the phase diagram. For the homogeneous case, the zeros of the oscillatory part are exactly at the positions where the fermion parity of the wavefunction for finite wires switches, a result previously obtained by other approaches [13, 14]. We therefore propose that our method can be further used to describe the fermion parity switches in the general inhomogeneous case, as well as to map the new non-topological phases found here into the magnetic phase diagram of its dual XY model [22, 23], when the transverse field or any other exchange coupling constant are equally modulated.

The Model.— Consider a Kitaev model periodically modulated, with site-dependent chemical potentials or hopping amplitudes along an enlarged unit-cell of size q repeated along the chain, while using periodic boundary conditions. Generically, for a system with N sites we can write such model Hamiltonian as $\mathcal{H} = \sum_{\ell=1}^{N/q} \mathcal{H}_\ell$, where

$$\mathcal{H}_\ell = \sum_{s=1}^q \mu_s c_{s,\ell}^\dagger c_{s,\ell} + \sum_{s=1}^{q-1} \left(-t_s c_{s,\ell}^\dagger c_{s+1,\ell} + \Delta_s c_{s,\ell} c_{s+1,\ell} \right) + \left(-t_q c_{q,\ell}^\dagger c_{1,\ell+1} + \Delta_q c_{q,\ell} c_{1,\ell+1} \right) + \text{H.c.} \quad (1)$$

It is a tight-binding model of spinless fermions with site-dependent chemical potentials (μ_s), hopping amplitudes (t_s) and p -wave superconducting pairings (Δ_s). For the site modulations we use either $\mu_s = \mu(1 + \lambda w_s)$ for the chemical potential or $t_s = t(1 + \lambda w_s)$ for the hopping amplitude, while $\Delta_s = \Delta$ is kept real and constant (absence of magnetic flux). λ is an extra parameter that provides the strength of the inhomogeneity and w_s are the spatial

distributions, which are taken as follows

$$w_s = \begin{cases} \delta_{s,1} & , \text{ a single-defect (S)} \\ \cos(2\pi s/q) & , \text{ commensurate (C)} \\ \cos(2\pi s\beta) & , \text{ incommensurate (I)} \end{cases} \quad (2)$$

where $\beta = (\sqrt{5} + 1)/2$ is the golden mean. The first of these distributions (S) needs no justification, while the others two (C,I) are in the class of Aubry-André or Harper potentials, useful for the study of disorder and superconductivity [24–26].

Using the Fourier transformation in each unit cell, $c_{s,\ell}^\dagger = \sqrt{q/N} \sum_k c_{s,k}^\dagger e^{ikq\ell}$, with $k \in (-\pi/q, \pi/q]$, the reduced Brillouin Zone, and through the well-known Bogoliubov-de Gennes (BdG) transformation [27] $\Psi_k = (c_{1,k}^\dagger, \dots, c_{q,k}^\dagger, c_{1,-k}, \dots, c_{q,-k})^T$, we can write down the Hamiltonian in momentum space as

$$\mathcal{H} = \frac{1}{2} \sum_k \Psi_k^\dagger \hat{H}_k \Psi_k = \frac{1}{2} \sum_k \Psi_k^\dagger \begin{pmatrix} \hat{V}_k & \hat{M}_k \\ \hat{M}_k^\dagger & -\hat{V}_{-k}^T \end{pmatrix} \Psi_k, \quad (3)$$

where \hat{V}_k and \hat{M}_k are $q \times q$ matrices whose non-zero elements are: $V_k^{s,s} = \mu_s$ for $s = 1, \dots, q$; $V_k^{s,s+1} = V_k^{s+1,s} = -t_s$ and $M_k^{s,s+1} = -M_k^{s+1,s} = -\Delta$ for $s = 1, \dots, q-1$; while $V_k^{q,1} = (V_k^{1,q})^* = -t_q e^{-ikq}$ and $M_k^{q,1} = (-M_k^{1,q})^* = -\Delta e^{-ikq}$ (see also [15]).

As long as the values of μ_s , t_s and Δ are real, this model has a time-reversal symmetry $\mathcal{T} = \mathcal{K}$ (\mathcal{K} takes the complex conjugate) that satisfies $\mathcal{T} \hat{H}_k \mathcal{T}^{-1} = \hat{H}_{-k}$, while the BdG transformation evinces a particle-hole symmetry of the model, characterized by $\mathcal{P} = \tau_x \mathcal{K}$ (where τ_x is the Pauli matrix acting on the particle-hole space) that satisfies $\mathcal{P} \hat{H}_k \mathcal{P}^{-1} = -\hat{H}_{-k}$. With these two operators, we can build a chiral operator $\mathcal{C} = \mathcal{T} \mathcal{P} = \tau_x$ that satisfies $\mathcal{C} \hat{H}_k \mathcal{C}^{-1} = -\hat{H}_k$. For the operators described above, we have $\mathcal{T}^2 = \mathcal{P}^2 = \mathcal{C}^2 = 1$, classifying this 1D system into the BDI symmetry class [28, 29], whose topological invariant is characterized by a \mathbb{Z} -index.

The topological invariant can be built from the Zak phase [30–32], which is the Berry phase for periodic fermion systems. To implement it, we first rotate the Hamiltonian (3) into a purely off-diagonal form

$$\Omega \hat{H}_k \Omega^\dagger = \begin{pmatrix} 0 & \hat{A}_k \\ \hat{A}_{-k}^\dagger & 0 \end{pmatrix}, \quad \hat{A}_k = \hat{V}_k + \hat{M}_k, \quad (4)$$

where $\Omega = e^{-i\pi\tau_y/4}$ is the unitary transformation and τ_y is the Pauli matrix acting on the particle-hole space. The topological index is thus the winding number of the eigenstates in the reduced Brillouin Zone, which for this kind of off-diagonal matrix is given by [31]

$$\mathcal{W} = -\frac{i}{\pi} \int_{k=0}^{\pi/q} \frac{dz_k}{z_k}, \quad \text{where} \quad z_k = \frac{\text{Det}(\hat{A}_k)}{|\text{Det}(\hat{A}_k)|}. \quad (5)$$

In this approach, the winding number ($\mathcal{W} \in \mathbb{Z}$) can be evaluated through the sign of the function $\text{Det}(\hat{A}_k)$ at the particle-hole symmetric k points, π/q and 0:

$$\mathcal{W} = \frac{1}{2} \left[\text{sgn}\{\text{Det}(\hat{A}_{\pi/q})\} - \text{sgn}\{\text{Det}(\hat{A}_0)\} \right]. \quad (6)$$

Thereby, for the Hamiltonian in (3) and (4) \mathcal{W} can only be ± 1 or 0 (Topological/Non-Topological, respectively).

Some selected results for the three spatial distributions (S,C,I) can be seen in Fig. 1. Apart from changes of the Topological/Non-Topological (T - NT) transition lines at $|\mu| = 2t$, we observe in all cases the emergence of non-topological compact domains (“bubbles”) around $\Delta/t = 0$. The number and shape of these bubbles depend on the cell size q , on the inhomogeneity strength λ , as well as on the spatial distribution. They look rather different when spatial modulations are applied either to the chemical potential or to the hopping amplitude (as can be seen from Fig. 1, left and right panels, respectively).

The Topological Invariant.– For the origin of the emerging bubbles in the topological phase diagram of the inhomogeneous cases, we consider some analytical aspects of the topological invariant. First, we rewrite the (real) function $\text{Det}(\hat{A}_\kappa)$, for $\kappa = 0$ and π/q , as

$$\text{Det}(\hat{A}_\kappa) = U(\mu, \Delta, q, \lambda) + \Lambda_\kappa(\Delta, q, \lambda), \quad (7)$$

where U is a κ -independent function that carries all the dependence on μ , and Λ_κ is the difference, in our (q, λ) scheme. According to expression (6), we observe that the system is topological ($\mathcal{W} \neq 0$) when U is within the region delimited by both Λ_κ (*viz.*: $\Lambda_0 < U < \Lambda_{\pi/q}$) and non-topological ($\mathcal{W} = 0$) otherwise. For cases where $\text{Det}(\hat{A}_\kappa) = 0$ expression (6) is undefined, though these points determine the *loci* of the T - NT transitions in the phase diagram, namely, the closure of the bulk gap. We have selected two featuring examples to display quantitatively this situation.

In Fig. 2 we plotted the homogeneous case (left panels) and the inhomogeneous single-defect model applied to the chemical potential (right panels), respectively. In the homogeneous case, we see in Fig. 2(c) that the function U oscillates between the two Λ_κ functions, for $|\mu| \leq 2t$, defining thus a topological phase in that region. Whereas in the single-defect case of Fig. 2(d), the function U goes out of these two limits because its oscillations are now enhanced by the presence of modulations. Beyond the topological phase, in the μ/t axis, the function U changes character and becomes unbounded in all cases. These trending features deserve further explanations.

Polynomial structure.– After detailed algebraic and numerical manipulations we found, in the homogeneous case ($\lambda = 0$), that the function U can be written as

$$U(\mu, \Delta, q, 0) = \left(\sqrt{1 - (\Delta/t)^2} \right)^q \bar{U}_H(\bar{\mu}, q), \quad (8)$$

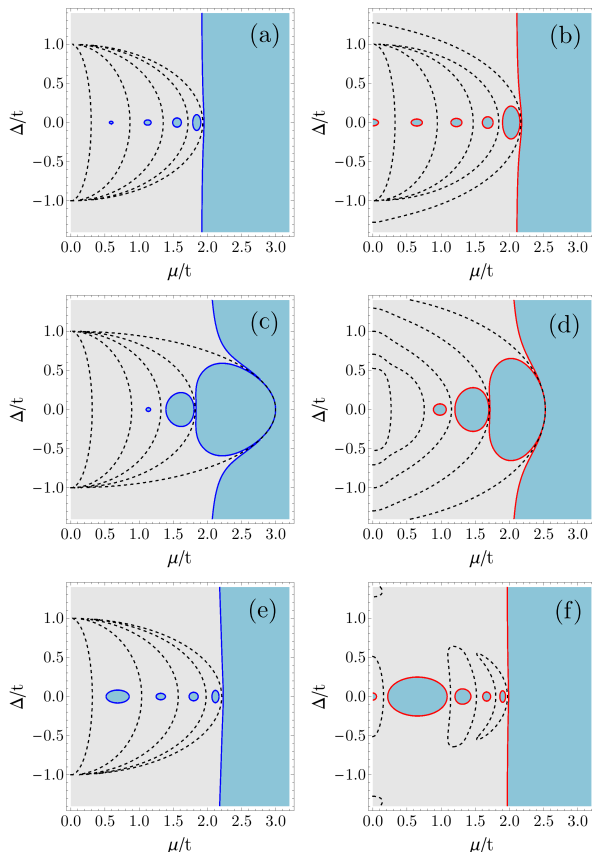


FIG. 1. Topological phase diagrams for modulated chemical potentials (left panels) and modulated hopping terms (right panels) in the (a,b) single-defect model, (c,d) commensurate and (e,f) incommensurate potentials. Topological (T) phases are the regions in light gray and Non-Topological (NT) phases are the zones in blue. Dark blue (left panels) and red (right panels) solid lines are the *loci* of the T - NT phase transitions, for which $\text{Det}(\hat{A}_k) = 0$. Dashed lines depicting ellipses are zeros of the oscillating function $U(\mu, \Delta, q, \lambda)$ given below. All diagrams are symmetric by changing $\mu \leftrightarrow -\mu$ and $\Delta \leftrightarrow -\Delta$. In all cases, we used $q = 10$ and $\lambda = 0.5$ in the enlarged unit-cell approach. Emerging features are the non-topological regions (“bubbles”) around the anisotropy line ($\Delta/t = 0$), and the bending of the Ising transition lines at $\mu \approx 2t$, notably for (c) and (d) cases. Case (f) will be discussed separately.

where $\bar{\mu} = \mu/\sqrt{1 - (\Delta/t)^2}$ is a scaled chemical potential, identical to the one found in DeGottardi *et al.* [9, 10], and $\bar{U}_H(\bar{\mu}, q)$ is described by a polynomial in $\bar{\mu}$ of degree q , restricted to integers $q \geq 2$

$$\bar{U}_H(\bar{\mu}, q) = \sum_{n=1}^q a_n^q \bar{\mu}^n, \quad (9)$$

whose coefficients $a_n^q \in \mathbb{Z}$ can be obtained through the following recurrence formula: $a_n^q = 1$ for all q , $a_1^q = \mp q$ (alternating) for q odd and $a_1^q = 0$ for q even, while for $1 < n < q$ we have $a_n^q = -a_n^{q-2} + a_{n-1}^{q-1}$ for $q-n$ even and $a_n^q = 0$ for $q-n$ odd. More details can be found in the Supplemental Material [33].

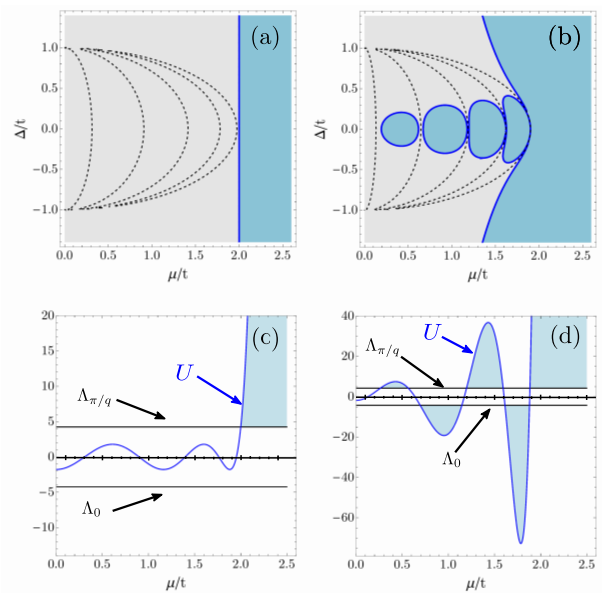


FIG. 2. Comparison of the homogeneous case (left panels, $\lambda = 0$) and the inhomogeneous single-defect case applied to the chemical potential (right panels, $\lambda = 10$). Topological regions are in gray, non-topological in blue. Dashed lines in phase diagrams (a) and (b) are zeros of the oscillating function U , whose outermost ones are very close to the ellipse $\bar{\mu} = 2t$, beyond which U is overdamped. Function U (blue curves) in (c) and (d) oscillates with q zeros until it crosses the Ising transition line close to $\mu/t = 2$. The main difference is that in (c), the homogeneous case, U is delimited by the two Λ_κ functions, while in (d) U goes beyond these two limits. This is the origin of the bubbles observed in the inhomogeneous case. These bubbles have alternating sign, corresponding to the wavefunction fermion parity. We have used $\Delta/t = 0.2$ in panels (c) and (d). For drawing purposes, we also shifted the vertical axis to get $U = 0$ as the mean of both Λ_κ functions.

As for the delimiting functions Λ_κ in Eq. (7), we found a useful relation in the form of a sum rule

$$\Lambda_{\pi/q} + \Lambda_0 = \left(\sqrt{1 - (\Delta/t)^2}\right)^q s^{1/2} (1 + s)^2, \quad (10)$$

where $s = (-1)^q$ and the factor $(1 + s)^2$ dictates that this sum is zero for q odd, while for q even the sum rule can be used to shift the zero. Using (10), we thus need to deal with only one of these polynomials. In this work, we study $\Lambda_0 = \Lambda_0(\Delta, q)$ which, for the homogeneous case, is given by an even polynomial in Δ

$$\Lambda_0(\Delta, q) = \sum_{n=0}^q b_n^q \Delta^n. \quad (11)$$

Some coefficients b_n^q are written in [33]. No simple recurrence formula for b_n^q has been found so far.

An interesting point is that the alternating polynomial \bar{U}_H in (9) has more than one root (in fact, q real roots), that yield an oscillatory structure for U inside the dome $\bar{\mu} = 2t$, that is, within the ellipse $(\mu/2t)^2 + (\Delta/t)^2 = 1$.

Outside this elliptical dome U has no more oscillations, as \bar{U}_H turns from an alternating to a positive overdamped polynomial in μ in that case. Such analytical behavior is a critical combination of the prefactor $(\sqrt{1 - (\Delta/t)^2})^q$ and the scaled $\bar{\mu} = \mu/\sqrt{1 - (\Delta/t)^2}$, that appear in Eq. (8). This result is consistent with those in [13, 14], about the positions of the fermion parity switches.

Modulated μ_s – When site modulations are applied to the chemical potential the sum rule (10) still applies, while the function U can be written now as

$$U(\mu, \Delta, q, \lambda) = \left(\sqrt{1 - (\Delta/t)^2}\right)^q (\bar{U}_H + \bar{U}_\lambda). \quad (12)$$

For the single-defect (S) case, the extra inhomogeneous contribution is linear on λ , that is $\bar{U}_\lambda = \lambda \bar{U}_S(\bar{\mu}, q)$, where \bar{U}_S is a polynomial like (9), with the same recurrence formula for the coefficients a_n^q , except that $a_1^q = \mp 1$ (alternating) for q odd and $a_1^q = 0$ for q even [33].

For the commensurate (C) and the incommensurate (I) potentials applied to μ_s , the extra contributions do not depend on Δ but are nonlinearly dependent on λ . That is, we have polynomials \bar{U}_λ in (12) written as $\bar{U}_C(\bar{\mu}, q, \lambda)$ and $\bar{U}_I(\bar{\mu}, q, \lambda)$, respectively, for which we have not found a simple recurrence formula yet. As an example, for $q = 3$ we have $\bar{U}_C(\bar{\mu}, 3, \lambda) = \frac{1}{4}\lambda^2(\lambda - 3)\bar{\mu}^3$. A similar expression for $\bar{U}_I(\bar{\mu}, 3, \lambda)$ can be found in [33].

Modulated t_s – Significant differences already begin when spatial modulations are applied to t_s , the hopping amplitude. For the single-defect (S) case, for example, we have now a function U described as

$$U(\mu, \Delta, q, \lambda) = \left(\sqrt{1 - (\Delta/t)^2}\right)^q \times \left(\bar{U}_H + \frac{\lambda(\lambda + 2)}{[1 - (\Delta/t)^2]} \tilde{U}_S\right), \quad (13)$$

while the sum rule for the Λ_κ functions is now given by

$$\Lambda_{\pi/q} + \Lambda_0 = \left(\sqrt{1 - (\Delta/t)^2}\right)^q s^{1/2} (1 + s)^2 \times \left(1 + \frac{\lambda(\lambda + 2)}{[1 - (\Delta/t)^2](1 + s)}\right). \quad (14)$$

In (13) we have $\tilde{U}_S = \tilde{U}_S(\bar{\mu}, q)$, which is a polynomial in $\bar{\mu}$ of degree $q \geq 3$, given by the same recurrence formula as in (9), except that the non-zero coefficients of the largest exponents are now $a_{q-2}^q = -1$ (*viz.*: $a_q^q = 0$ for all q). We notice in (13) and (14) the extra terms in $\lambda(\lambda + 2)$, which depend also on Δ . This contribution expands the dome of the oscillations of the function U beyond the limits $\Delta/t = \pm 1$, as is indeed observed in Fig. 1(b).

For the commensurate (C) and the incommensurate (I) potentials applied to the hopping, on the other hand, a general expression for the function U is as follows

$$U(\mu, \Delta, q, \lambda) = \left(\sqrt{1 - (\Delta/t)^2}\right)^q \bar{U}_H + \tilde{U}_\lambda. \quad (15)$$

The corresponding inhomogeneous \tilde{U}_λ terms, namely, $\tilde{U}_C = \tilde{U}_C(\mu, \Delta, q, \lambda)$ or $\tilde{U}_I = \tilde{U}_I(\mu, \Delta, q, \lambda)$, respectively, are now polynomials in μ and Δ which cannot be simply factored as in (12) or in (13). The latter two cases in (15) are examples where the above elliptical description does not apply anymore, as can be inferred from Figs. 1(d) and (f). Closed relations for terms \tilde{U}_C , \tilde{U}_I or Λ_κ in this modulated t_s case were not yet found, although there seems to be a fractional polynomial description for some of them. Examples for $q = 3$ and 5 may be seen in [33], suggesting that the latter is true.

Summary. – In summary, we have studied the effect of inhomogeneities in the 1D p -wave Kitaev model, for which we constructed an integer polynomial description for the topological invariant using an enlarged-unit cell approach. We applied the method to three fixed spatial distributions (S,C,I), although it can be easily expanded to more general cases. A comparative study was made for modulated chemical potential and hopping terms, finding very clear differentiations. The oscillatory behavior of the polynomial function U takes account of most of the topological features of the model, not only of the origin of the emerging non-topological bubbles close to the anisotropy line ($\Delta = 0$), but also of the exact positions of the ground-state fermion parity switches for homogeneous finite wires, which are given by the elliptical curves $\bar{\mu} = 2t \cos(\pi p/(q+1))$, where $p = 1, 2, \dots, [q/2]$; see more details in [13, 14].

The fact that our periodic boundary bulk results are consistent with those for open boundary systems, with edge Majorana fermions, obtained otherwise through the large size limit of the transfer matrix approach, is a consequence of the *bulk-edge correspondence*. Therefore, with this validity test we propose to use these results also for the inhomogeneous cases. The new zeros of the shifted function U , like those seen in the examples of Figs. 1 and 2, should be the positions of the new fermion parity switches in those cases.

Moreover, as a byproduct, since the Kitaev chain is exactly mapped into the XY model through a Jordan-Wigner transformation [22, 23], we thus hope that other authors would be willing to observe compact paramagnetic bubbles into the ferromagnetic region of the inhomogeneous XY model, as well. What remains to verify is whether the oscillations of the spin correlation function for the XY model would be at the same oscillatory region of the function U , as it is in the homogeneous case.

Acknowledgments. – We acknowledge Drs. Germán Sierra, J. Carlos Egues, Raul Santos, and S. Valencia for enlightening discussions. This work was financially supported by the Brazilian agencies CNPq and CAPES.

* marcos.perez@ufrgs.br

- [1] J. Alicea, Rep. Prog. Phys. **75**, 076501 (2012).
- [2] C. Beenakker, Annu. Rev. of Condens. Matter Phys. **4**, 113 (2013).
- [3] S. R. Elliott and M. Franz, Rev. Mod. Phys. **87**, 137 (2015).
- [4] V. Mourik, K. Zuo, S. M. Frolov, S. R. Plissard, E. P. A. M. Bakkers, and L. P. Kouwenhoven, Science **336**, 1003 (2012).
- [5] M. Z. Hasan and C. L. Kane, Rev. Mod. Phys. **82**, 3045 (2010).
- [6] S. Das Sarma, M. Freedman, and C. Nayak, NPJ Quantum Information **1**, 15001 (2015).
- [7] A. Y. Kitaev, Physics-Uspekhi **44**, 131 (2001).
- [8] L.-J. Lang and S. Chen, Phys. Rev. B **86**, 205135 (2012).
- [9] W. DeGottardi, D. Sen, and S. Vishveshwara, Phys. Rev. Lett. **110**, 146404 (2013).
- [10] W. DeGottardi, M. Thakurathi, S. Vishveshwara, and D. Sen, Phys. Rev. B **88**, 165111 (2013).
- [11] I. Adagideli, M. Wimmer, and A. Teker, Phys. Rev. B **89**, 144506 (2014).
- [12] R. Wakatsuki, M. Ezawa, Y. Tanaka, and N. Nagaosa, Phys. Rev. B **90**, 014505 (2014).
- [13] S. Hegde, V. Shivamoggi, S. Vishveshwara, and D. Sen, New Journal of Physics **17**, 053036 (2015).
- [14] S. S. Hegde and S. Vishveshwara, Phys. Rev. B **94**, 115166 (2016).
- [15] Y. Gao, T. Zhou, H. Huang, and R. Huang, Scientific Report **5**, 17049 (2015).
- [16] J. Alicea, Phys. Rev. B **81**, 125318 (2010).
- [17] G. Ortiz, J. Dukelsky, E. Cobanera, C. Eсеbbag, and C. Beenakker, Phys. Rev. Lett. **113**, 267002 (2014).
- [18] R. Queiroz, E. Khalaf, and A. Stern, Phys. Rev. Lett. **117**, 206405 (2016).
- [19] L. Fidkowski and A. Kitaev, Phys. Rev. B **81**, 134509 (2010).
- [20] E. Tang and X.-G. Wen, Phys. Rev. Lett. **109**, 096403 (2012).
- [21] N. M. Gergs, L. Fritz, and D. Schuricht, Phys. Rev. B **93**, 075129 (2016).
- [22] E. Lieb, T. Schultz, and D. Mattis, Ann. Phys. (N.Y.) **16**, 407 (1961).
- [23] J. E. Bunder and R. H. McKenzie, Phys. Rev. B **60**, 344 (1999).
- [24] S. Aubry and G. André, Ann. Israel Phys. Soc. **3**, 133 (1980).
- [25] X. Cai, L.-J. Lang, S. Chen, and Y. Wang, Phys. Rev. Lett. **110**, 176403 (2013).
- [26] X. Cai, J. Phys.: Condens. Matter **26**, 155701 (2014).
- [27] P. De Gennes, *Superconductivity of Metals and Alloys*, Advanced Books Classics Series (Westview Press, 1999).
- [28] A. Altland and M. R. Zirnbauer, Phys. Rev. B **55**, 1142 (1997).
- [29] A. P. Schnyder, S. Ryu, A. Furusaki, and A. W. W. Ludwig, Phys. Rev. B **78**, 195125 (2008).
- [30] J. Zak, Phys. Rev. Lett. **62**, 2747 (1989).
- [31] S. Tewari and J. D. Sau, Phys. Rev. Lett. **109**, 150408 (2012).
- [32] D. Xiao, M.-C. Chang, and Q. Niu, Rev. Mod. Phys. **82**, 1959 (2010).
- [33] See Supplemental Material at <http://link.aps.org/supplemental/PhysRevLett> for more details.
-

Supplemental material for “Polynomial Description of the Topological Invariant in Inhomogeneous Superconducting Wires”

In this supplemental material we present some analytical details and tables of the polynomial description of the topological invariant in the inhomogeneous Kitaev chain.

THE TOPOLOGICAL INVARIANT

For the inhomogeneous Kitaev chain, we can write the model Hamiltonian as $\mathcal{H} = \sum_{\ell=1}^{N/q} \mathcal{H}_\ell$, with

$$\mathcal{H}_\ell = \sum_{s=1}^q \mu_s c_{s,\ell}^\dagger c_{s,\ell} + \sum_{s=1}^{q-1} \left[-t_s c_{s,\ell}^\dagger c_{s+1,\ell} + \Delta_s c_{s,\ell}^\dagger c_{s+1,\ell}^\dagger \right] - t_q c_{q,\ell}^\dagger c_{1,\ell+1} + \Delta_q c_{q,\ell}^\dagger c_{1,\ell+1}^\dagger + \text{H.c.} \quad (\text{S1})$$

where an enlarged unit-cell approach of size q was used, with periodic boundary conditions. Because of the particle-hole symmetry, this Hamiltonian can be written, in momentum space, through a Bogoliubov-de Gennes transformation $\Psi_k = (c_{1,k}^\dagger, \dots, c_{q,k}^\dagger, c_{1,-k}, \dots, c_{q,-k})^T$, plus a rotation to an off-diagonal form, as shown below

$$\mathcal{H} = \frac{1}{2} \sum_k \Psi_k^\dagger \begin{pmatrix} 0 & \hat{A}_k \\ \hat{A}_{-k}^T & 0 \end{pmatrix} \Psi_k. \quad (\text{S2})$$

In such a representation, the $q \times q$ \hat{A}_k matrix, with $k \in (-\pi/q, \pi/q]$, is written as a sum of an hermitian plus an antisymmetric matrix, respectively: $\hat{A}_k = \hat{V}_k + \hat{M}_k$, as seen from expressions (3) and (4) of the main text. As an example, for $q = 5$ we have the following matrix components

$$\hat{V}_k = \begin{pmatrix} \mu_1 & -t_1 & 0 & 0 & -t_5 e^{i5k} \\ -t_1 & \mu_2 & -t_2 & 0 & 0 \\ 0 & -t_2 & \mu_3 & -t_3 & 0 \\ 0 & 0 & -t_3 & \mu_4 & -t_4 \\ -t_5 e^{-i5k} & 0 & 0 & -t_4 & \mu_5 \end{pmatrix}; \quad \hat{M}_k = \begin{pmatrix} 0 & -\Delta_1 & 0 & 0 & \Delta_5 e^{i5k} \\ \Delta_1 & 0 & -\Delta_2 & 0 & 0 \\ 0 & \Delta_2 & 0 & -\Delta_3 & 0 \\ 0 & 0 & \Delta_3 & 0 & -\Delta_4 \\ -\Delta_5 e^{-i5k} & 0 & 0 & \Delta_4 & 0 \end{pmatrix}. \quad (\text{S3})$$

Spatial modulations we used are of type $\mu_s = \mu(1 + \lambda w_s)$ for the chemical potential or $t_s = t(1 + \lambda w_s)$ for the hopping term, while all Δ terms are taken as positive real constants. The profiles of the modulations w_s are given in Eq. (2) of the main text, λ is the strength of the inhomogeneity, and from now on the hopping term will be taken as the energy scale ($t = 1$).

Realizing that this 1D model is in the BDI symmetry class, then it has a topological index given by the winding number, which is of type \mathbb{Z} , and whose expression is given by

$$\mathcal{W} = -\frac{i}{\pi} \int_{k=0}^{\pi/q} \frac{dz_k}{z_k}, \quad \text{where} \quad z_k = e^{i\theta_k} = \frac{\text{Det}(\hat{A}_k)}{|\text{Det}(\hat{A}_k)|}. \quad (\text{S4})$$

In our approach, this can be evaluated through $\mathcal{W} = \frac{1}{2} [\text{sgn}\{\text{Det}(\hat{A}_{\pi/q})\} - \text{sgn}\{\text{Det}(\hat{A}_0)\}]$, at the particle-hole symmetric k points, π/q and 0. Since we have $\hat{A}_k = (\hat{A}_{-k})^*$, then $\text{Det}(\hat{A}_k)$ is a real function at the extreme points, 0 and π/q . The regions in the μ - Δ phase diagram are classified as Topological ($\mathcal{W} \neq 0$) or Non-Topological ($\mathcal{W} = 0$), according to this recipe. Therefore, our attention is focused on the function $\text{Det}(\hat{A}_k)$, which is intrinsically a polynomial in μ and Δ of degree q . As such, we propose to split it at the extreme k points in the following way

$$\text{Det}(\hat{A}_\kappa) = U(\mu, \Delta, q, \lambda) + \Lambda_\kappa(\Delta, q, \lambda), \quad (\text{S5})$$

where κ is either 0 or π/q . Function U contains explicitly all the μ -dependence and the functions Λ_κ are defined by the difference. Moreover, U is an oscillatory function which has q real roots along the μ axis within the topological region, which for the homogeneous case is given by $|\mu| \leq 2t$, and it is unbounded beyond that limit. On the other hand, functions Λ_κ act as limiting values for the function U in the evaluation of the winding number.

THE HOMOGENEOUS CASE

Let us describe first functions U and Λ_κ for the homogeneous case ($\lambda = 0$). U is a polynomial in μ of degree q whose coefficients depend on Δ . The dependence on Δ can be factorized as follows

$$U(\mu, \Delta, q, 0) = \left(\sqrt{1 - \Delta^2}\right)^q \bar{U}_H(\bar{\mu}, q), \quad (\text{S6})$$

where $\bar{\mu} = \mu/\sqrt{1 - \Delta^2}$ is a scaled chemical potential and \bar{U}_H is a polynomial in $\bar{\mu}$ whose coefficients are independent of Δ

$$\bar{U}_H(\bar{\mu}, q) = \sum_{n=1}^q a_n^q \bar{\mu}^n. \quad (\text{S7})$$

Some of these coefficients a_n^q are given in Table I. They can be obtained through the following [recurrence formula](#): $a_q^q = 1$ for all q , $a_1^q = \mp q$ (alternating) for q odd and $a_1^q = 0$ for q even, while for $1 < n < q$ we have $a_n^q = a_{n-1}^{q-1} - a_n^{q-2}$ for $q - n$ even and $a_n^q = 0$ for $q - n$ odd. We notice that the nonzero integer coefficients of this polynomial have alternating signs for each q . The oscillatory behavior of this function is due to this fact. It is easily seen that U , as a function of μ is symmetric for q even and antisymmetric for q odd, while it is always symmetric with respect to Δ .

q	n									
	1	2	3	4	5	6	7	8	9	10
2	0	1	0	0	0	0	0	0	0	0
3	-3	0	1	0	0	0	0	0	0	0
4	0	-4	0	1	0	0	0	0	0	0
5	5	0	-5	0	1	0	0	0	0	0
6	0	9	0	-6	0	1	0	0	0	0
7	-7	0	14	0	-7	0	1	0	0	0
8	0	-16	0	20	0	-8	0	1	0	0
9	9	0	-30	0	27	0	-9	0	1	0
10	0	25	0	-50	0	35	0	-10	0	1

TABLE I. Some coefficients a_n^q of the polynomial \bar{U}_H in the homogeneous case.

For the delimiting functions Λ_κ , on the other hand, a useful relation is given by the [sum rule](#)

$$\Lambda_{\pi/q} + \Lambda_0 = \left(\sqrt{1 - \Delta^2}\right)^q s^{1/2}(1 + s)^2, \quad (\text{S8})$$

where $s = (-1)^q$ and the term $(1 + s)^2$ forces this sum rule to zero for q odd. Such relation restricts our study to one of these polynomials. In this work we deal with $\Lambda_0(\Delta, q) = \sum_{n=0}^q b_n^q \Delta^n$ which, in this case, is an even polynomial in Δ ($b_n^q = 0$ for n odd), whose coefficients are given in Table II.

q	n				
	0	2	4	6	8
2	2	0	0	0	0
3	1	3	0	0	0
4	0	8	0	0	0
5	1	10	5	0	0
6	2	12	18	0	0
7	1	21	35	7	0
8	0	32	64	32	0
9	1	36	126	84	9
10	2	40	220	200	50

TABLE II. Some coefficients $-b_n^q/2$ of the polynomial $\Lambda_0(\Delta, q)$ in the homogeneous case.

Let us see the region $\Delta > 1$. The prefactor $(\sqrt{1 - \Delta^2})^q$ in Eq. (S6) is then purely imaginary for q odd and a negative number for q even. The effect of this over U is to change signs of all negative coefficients a_n^q , as seen on Table I. These change of signs cause U to turn from an oscillatory to an overdamped polynomial with all coefficients positive. Consequently, for $\Delta > 1$ the function U does not oscillate anymore in the homogeneous case.

The oscillatory behavior of U for $|\Delta| < 1$, on the other hand, can be summarized as follows: the function U has an oscillatory part and an overdamped part. The oscillatory part of the U -shifted is limited by $\bar{\mu} = 2$. This constraint describes an ellipse in the parameter space, written as $(\mu/2)^2 + \Delta^2 = 1$, wherein the function U is oscillatory and outside is just an overdamped function.

MODULATED CHEMICAL POTENTIAL

When spatial distributions are applied to the chemical potential, the coefficients of the polynomial function U depend now on the disorder strength λ , while the delimiting functions Λ_κ are not affected by λ , since the sum rule is the same as in the homogeneous description.

Single-defect case

When we apply the single-defect spatial distribution to the chemical potential, the function $U(\mu, \Delta, q, \lambda)$ can be written as

$$U(\mu, \Delta, q, \lambda) = \left(\sqrt{1 - \Delta^2}\right)^q (\bar{U}_H + \bar{U}_\lambda), \quad (\text{S9})$$

where \bar{U}_H is the polynomial for the homogeneous case and $\bar{U}_\lambda = \lambda \bar{U}_S(\bar{\mu}, q)$ is a polynomial in $\bar{\mu}$ of degree q , linearly dependent in λ , whose coefficients are given in Table III. These coefficients a_n^q have the same recurrence formula as in Eq. (S7), except that for $a_1^q = \mp 1$ (alternating) for q odd and $a_1^q = 0$ for q even. As \bar{U}_λ in Eq. (S9) is linear in λ , the coefficients of \bar{U}_S in Table III are λ -independent.

q	n									
	1	2	3	4	5	6	7	8	9	10
2	0	1	0	0	0	0	0	0	0	0
3	-1	0	1	0	0	0	0	0	0	0
4	0	-2	0	1	0	0	0	0	0	0
5	1	0	-3	0	1	0	0	0	0	0
6	0	3	0	-4	0	1	0	0	0	0
7	-1	0	6	0	-5	0	1	0	0	0
8	0	-4	0	10	0	-6	0	1	0	0
9	1	0	-10	0	15	0	-7	0	1	0
10	0	5	0	-20	0	21	0	-8	0	1

TABLE III. Some coefficients a_n^q of the polynomial $\bar{U}_S(\bar{\mu}, q)$ for the single-defect case.

Commensurate and incommensurate potential

For these two spatial distributions, the function U can be written as in Eq. (S9), where \bar{U}_λ are nonlinear polynomials in λ and $\bar{\mu}$ of degree q that are independent of Δ . We have not found recurrence formulas for them so far. We can give examples for $q = 3$. For the (C) commensurate case, we have

$$\bar{U}_C(\bar{\mu}, q = 3, \lambda) = \frac{1}{4} \lambda^2 (\lambda - 3) \bar{\mu}^3, \quad (\text{S10})$$

and for the (I) incommensurate case

$$\begin{aligned} \bar{U}_I(\bar{\mu}, q = 3, \lambda) = & - [\cos(2\pi\beta) + \cos(4\pi\beta) + \cos(6\pi\beta)] \lambda (\bar{\mu} - \bar{\mu}^3) \\ & + [\cos(2\pi\beta) \cos(4\pi\beta) + \cos(2\pi\beta) \cos(6\pi\beta) + \cos(4\pi\beta) \cos(6\pi\beta)] \lambda^2 \bar{\mu}^3 \\ & + [\cos(2\pi\beta) \cos(4\pi\beta) \cos(6\pi\beta)] \lambda^3 \bar{\mu}^3. \end{aligned} \quad (\text{S11})$$

MODULATED HOPPING AMPLITUDE

We now turn to the situation when the spatial distributions are applied to the hopping amplitude. Functions U and Λ_κ depend now on the disorder strength λ and on the kind of distribution applied. Many things are different now. The previous sum rule, for example, is not valid anymore.

Single-defect case

When we apply the single-defect spatial distribution to the hopping, the function U can be written as

$$U(\mu, \Delta, q, \lambda) = \left(\sqrt{1 - \Delta^2}\right)^q \left(\bar{U}_H + \frac{\lambda(\lambda + 2)}{1 - \Delta^2} \tilde{U}_S\right) \quad (\text{S12})$$

where $\tilde{U}_S = \tilde{U}_S(\bar{\mu}, q)$ is a polynomial function, whose coefficients are independent of the disorder strength λ and of the pairing Δ . Some of them are given in Table IV. We did not find disorder effect for $q = 2$. This polynomial has the same recurrence formula as in Eq. (S7), except that the non-zero coefficients of the largest exponents are now $a_{q-2}^q = -1$ (*viz.*: $a_q^q = 0$ for all q).

q	n							
	1	2	3	4	5	6	7	8
3	-1	0	0	0	0	0	0	0
4	0	-1	0	0	0	0	0	0
5	2	0	-1	0	0	0	0	0
6	0	3	0	-1	0	0	0	0
7	-3	0	4	0	-1	0	0	0
8	0	-6	0	5	0	-1	0	0
9	4	0	-10	0	6	0	-1	0
10	0	10	0	-15	0	7	0	-1

TABLE IV. Some coefficients a_n^q of the polynomial $\tilde{U}_S(\bar{\mu}, q)$ for the single-defect case.

Different from the previous cases, the sum rule of the Λ_κ functions is now λ -dependent and it is given by

$$\Lambda_{\pi/q}(\Delta, q, \lambda) + \Lambda_0(\Delta, q, \lambda) = \left(\sqrt{1 - \Delta^2}\right)^q s^{1/2}(1 + s)^2 \left(1 + \frac{\lambda(\lambda + 2)}{(1 - \Delta^2)(1 + s)}\right) \quad (\text{S13})$$

The polynomial $\Lambda_0(\Delta, q, \lambda) = \sum_{n=0}^q b_n^q \Delta^n$ is an even polynomial in Δ of degree q , whose coefficients are nonlinear in λ , as can be seen from Table V.

q	n			
	0	2	4	6
2	$-(2 + \lambda)^2$	0	0	0
3	$-2(1 + \lambda)$	$-2(3 + \lambda)$	0	0
4	λ^2	$-(4 + \lambda)^2$	0	0
5	$-2(1 + \lambda)$	$-4(5 + 3\lambda)$	$-2(5 + \lambda)$	0
6	$-(2 + \lambda)^2$	$-2(12 + 8\lambda - \lambda^2)$	$-(6 + \lambda)^2$	0
7	$-2(1 + \lambda)$	$-6(7 + 5\lambda)$	$-10(7 + 3\lambda)$	$-2(7 + \lambda)$
8	λ^2	$-(64 + 48\lambda + 3\lambda^2)$	$-(128 + 64\lambda - 3\lambda^2)$	$-(8 + \lambda)^2$

TABLE V. Some coefficients $-b_n^q/2$ of the polynomial $\Lambda_0(\Delta, q, \lambda)$ for the single-defect case.

Commensurate and incommensurate potentials

Different from the above descriptions in (S9) and (S12), the function U cannot be factorized in these two latter cases. Therefore, the modulation effect can be simply written as

$$U(\mu, \Delta, q, \lambda) = \left(\sqrt{1 - \Delta^2}\right)^q \bar{U}_H + U_i \quad (\text{S14})$$

where $U_i = U_i(\mu, \Delta, q, \lambda)$ and $i = \{C, I\}$, respectively. There are no recurrence formulae found for these cases yet. An example for $q = 5$, and for the (C) commensurate case, is given by

$$U_C(\mu, \Delta, q = 5, \lambda) = -5\Delta^2\lambda^2\mu + \frac{5}{32}\sqrt{5}\lambda^4\mu + \frac{35\lambda^4\mu}{32} - \frac{5\lambda^2\mu^3}{2} - \frac{5}{2}\sqrt{5}\lambda^2\mu + \frac{5\lambda^2\mu}{2}, \quad (\text{S15})$$

while for the polynomial $\Lambda_0 = \Lambda_{0,H} + \Lambda_{0,C}$, we have the following

$$\Lambda_{0,C}(\Delta, q = 5, \lambda) = \frac{1}{8}\lambda^2(20 - 5\lambda^2 - \lambda^3 + 60\Delta^2), \quad (\text{S16})$$

where $\Lambda_{0,H}$ corresponds to the Λ_0 of the homogeneous case, in Table II. Similarly, as an example for $q = 3$, and for the (I) incommensurate case, we have found the following expression

$$U_I(\mu, \Delta, q = 3, \lambda) = -[2\lambda(\cos(2\pi\beta) + \cos(4\pi\beta) + \cos(6\pi\beta)) + \lambda^2(\cos^2(2\pi\beta) + \cos^2(4\pi\beta) + \cos^4(6\pi\beta))] \mu, \quad (\text{S17})$$

where $\beta = (\sqrt{5} + 1)/2$ is the golden mean, while for the polynomial $\Lambda_0 = \Lambda_{0,H} + \Lambda_{0,I}$, with

$$\begin{aligned} \Lambda_{0,I}(\Delta, q = 3, \lambda) = & -2\lambda[\cos(2\pi\beta) + \cos(4\pi\beta) + \cos(6\pi\beta)](1 + \Delta^2) \\ & -2\lambda^2[\cos(2\pi\beta)\cos(4\pi\beta) + \cos(2\pi\beta)\cos(6\pi\beta) + \cos(4\pi\beta)\cos(6\pi\beta)] \\ & -2\lambda^3[\cos(2\pi\beta)\cos(4\pi\beta)\cos(6\pi\beta)], \end{aligned} \quad (\text{S18})$$

where we have decided to keep the harmonics $\cos(n\pi\beta)$ in the latter incommensurate cases to show the structure of such polynomials.